

1 Immunomodulation of exopolysaccharide produced by *Lacticaseibacillus*
2 *rhamnosus* ZFM216 in cyclophosphamide-induced immunosuppressed
3 mice by modulating gut microbiota

4 Liang Chen,^a Dong Wang,^b Wei Liu,^c Shaobo Zhou,^{d, a} Qing Gu,^a Tao Zhou*^a

5 ^a. Key Laboratory for Food Microbial Technology of Zhejiang Province, School of Food
6 Science and Biotechnology, Zhejiang Gongshang University, Xiasha, Hangzhou, Zhejiang,
7 310018, P. R. China

8 ^b. Zhejiang Chemtrue Bio-Pharm Co., Ltd. Xiasha, Hangzhou, Zhejiang, 310018, P. R. China

9 ^c. Institute of Plant Protection and Microbiology, Zhejiang Academy of Agricultural Sciences,
10 Hangzhou, Zhejiang, PR China

11 ^d. School of Science, Faculty of Engineering and Science, University of Greenwich, Central
12 Avenue, Chatham ME4 4TB, UK

13

14 Runing title: Exopolysaccharide improve immunomodulatory effect

15 *Corresponding authors. Tel: (+86) 571 28008976. E-mail address: taozhou@zjgsu.edu.cn (T.
16 Zhou), ORCID: 0000-0003-4510-3639 (Tao Zhou)

17 **ABSTRACT**

18 This study investigated the immunoregulatory activity of exopolysaccharides (EPS) produced
19 by *Lacticaseibacillus rhamnosus* ZFM216 in immunosuppressed mice induced by
20 cyclophosphamide (CTX). The results showed that EPS treatment effectively improved the
21 body weight, immune organ index and splenic lymphocyte proliferation. EPS also mitigated
22 the damage of immune organs, restored intestinal morphology, and regulated the levels of
23 serum hemolysin and cytokines (e.g. TNF- α , INF- γ and IL-10). EPS promoted the release of
24 NO, TNF- α , IL-1 β , and IL-6 in RAW 264.7 cells, however, such effect was inhibited in the
25 presence of inhibitors of TLR4 and MAPKs signaling pathways-related proteins, confirming
26 that EPS achieved the immunomodulation by activating these two signaling pathways.
27 Additionally, EPS, as a prebiotic, effectively improved the diversity of microbial communities,
28 regulated the relative abundance of dominant microbial communities, restored CTX-induced
29 gut microbiota dysbiosis, and promoted the production of short chain fatty acids (SCFAs) in
30 the gut of mice. Thus, immunoregulatory effect of EPS could be attributed to its good ability
31 to modulate the gut microbiota. EPS produced by *L. rhamnosus* ZFM216 has promising
32 application as an ingredient of functional foods due to its potent probiotic effect.

33

34 **Keywords:** Exopolysaccharides; Gut microbiota; Immunomodulatory effect

35 1. Introduction

36 Lactic acid bacteria are generally considered safe for consumption due to their pollution-
37 free, safe, probiotic, and economic characteristics [1]. Their metabolites, exopolysaccharides
38 (EPS), are also considered non-toxic, and have attracted considerable attention due to their
39 numerous excellent biological activities, such as antioxidant, antitumor, and anti-inflammatory
40 effects [2–5]. Studies have revealed that EPSs possess potent immune regulatory activity and
41 are explored as food supplements or dietary applications [6]. Generally, non-starch
42 polysaccharides are difficult to directly absorb by the human body, but can be decomposed and
43 utilized by the gut microbiota, ultimately leading to changes in the composition of the gut
44 microbiota, bacterial metabolic active substances, and the gut cavity environment [7–9]. Wu et
45 al. reported that EPS produced by *Lactobacillus plantarum* YW11 improved immune response
46 by restoring the diversity of gut microbiota, increasing the butyric acid content in the intestine,
47 and increasing the relative abundance of *Roseburia*, *Ruminococcus*, and *Blautia* [10].

48 The immune system, composed of immune organs, immune cells and immune molecules
49 [11,12], is crucial for the body to execute immune responses and exert immune functions
50 [13,14]. It can protect the host from pathogenic bacteria, coordinate with other systems in the
51 body, and maintain the stability of the internal environment [15–17]. The fast-paced life, intense
52 work pressure, and irregular schedule lead to immune disorders in the human body, which is
53 closely related to many chronic diseases, such as aging, tumors, diabetes, and hypertension
54 [17–20]. At present, such diseases are usually treated with chemical drugs, but long-term and
55 large dosage use of chemical drugs will cause many side effects, such as anemia, edema,
56 indigestion, and gastrointestinal toxicity [21]. Therefore, to counteract the adverse reactions

57 caused by the chemical drugs and improve the therapeutic efficacy, there is a demand to
58 develop natural products-based functional foods or drugs with immunomodulatory effects. To
59 this end, polysaccharides have received considerable interest. For instance, Alhagi honey
60 polysaccharides, yam polysaccharides, and pectins all were reported to attenuate intestinal
61 injury and immune suppression in cyclophosphamide (CTX)-induced mice [22–24].

62 Recently, a bacterial strain was isolated from fresh milk in our laboratory and identified
63 as *Lacticaseibacillus rhamnosus* ZFM216. This bacterium was found to grow well in a newly
64 developed culture medium; use of this culture medium not only avoids interference of EPS
65 analysis from the polysaccharides in the culture medium components, but also allows the
66 bacterium to have an increased EPS production [25]. As the culture conditions of LABs might
67 also affect the structure of the yielding EPSs [26], and bioactivities of polysaccharides are
68 greatly affected by their structural properties, the EPS produced by *L. rhamnosus* ZFM216
69 under the growth conditions using the new culture medium results in its uniqueness and novelty.
70 In our previous study, this EPS was found to possess excellent immune ability *in vitro* [25]. We
71 hypothesize that this EPS could possess considerable immunomodulatory effects *in vivo*, which
72 makes it have potential applications in food and medicine. Herein, the immunomodulatory
73 effect of this EPS based on a CTX-induced immunosuppressive mouse model is described.
74 Analyses of short-chain fatty acids (SCFAs) and microbial community structure in the mouse
75 intestine, and analysis of effects of EPS on signaling pathways in RAW264.7 macrophages
76 using specific protein inhibitor method, were also conducted to reveal the underlying
77 mechanism of immune regulation by the EPS.

78

79 **2. Materials and methods**

80 *2.1 Materials and reagents*

81 *Lacticaseibacillus rhamnosus* ZFM216 was isolated from fresh milk, stored in key
82 laboratory for food microbial technology of Zhejiang Province, and deposited in the China
83 Center for Type Culture Collection (CCTCC) under accession number NO. CCTCC M
84 2020325. CTX was purchased from Macklin Biochemical Co. Ltd. (Shanghai, China).
85 Lentinan and RPMI-1640 medium were provided by Yuanye Bio-Technology Co. Ltd.
86 (Shanghai, China). Indian ink was purchased from Ruji Bio-Technology Development Co. Ltd.
87 (Shanghai, China). 3-(4,5-Dimethylthiazol-2-yl)-2,5-diphenyltetrazolium bromide (MTT) kit
88 was purchased from Carnoss Technology Co. Ltd. (Wuhan, China). Sheep red blood cell
89 (SRBC) was purchased from Bersee Bio-Technology Co. Ltd. (Beijing, China). Mouse
90 lymphocyte isolate was purchased from Dakewe Bio-Technology Co. Ltd. (Shenzhen, China).
91 ELISA kits for the mouse hemolysin, IL-10, INF- γ , and TNF- α assays were supplied by Yeasen
92 Bio-Technology Co. Ltd (Shanghai, China). Acetic acid, propionic acid, isobutyric acid,
93 butyric acid, isovaleric acid, and valeric acid were obtained from Sigma Chemical Co. Ltd. (St.
94 Louis, Mo, USA).

95 EPS from *L. rhamnosus* ZFM216 was prepared and isolated according to our previously
96 published method [25]. The total sugar, protein and uronic acid contents in EPS were 70.06%,
97 1.44% and 17.74%, respectively; EPS was composed of guluronic acid, mannuronic acid,
98 mannose, ribose, rhamnose, galacturonic acid, glucose, xylose, galactose and arabinose with
99 the molar ratios of 95.2 : 1 : 19.2 : 1.4 : 3.3 : 1.2 : 106.8 : 1.4 : 5.9 : 13.6; the molecular weight
100 of EPS was 19.9 kDa [25].

101 *2.2 Animals and experimental design*

102 All animal tests were conducted at the Experimental Animal Center of Hangzhou Normal
103 University and all procedures involving animals complied with the requirement of the National
104 Research Council's Guide for the Care and Use of Laboratory Animals
105 (<https://grants.nih.gov/grants/olaw/guide-for-the-care-and-use-of-laboratory-animals.pdf>) and
106 were approved by the Committee for Animal Studies and the Committee on Care and Use of
107 Laboratory Animals of Hangzhou Normal University (License No. SYSK(zhe)2021-0029).
108 Sixty specific pathogen-free female Kunming mice (20.0 ± 2.0 g) could eat and drink freely
109 and were kept at 22 ± 2 °C, 12/12 h light/dark period, and $55 \pm 10\%$ relative humidity for 1-
110 week acclimation. The model establishment and treatment plan were according to Huang et
111 al.'s method with slight modifications [23]. The grouping and experimental design of animal
112 tests are depicted in Fig. 1. The mice were stochastically divided into the normal control group
113 (NC), model group (MC), lentinan positive group (PC), EPS low, middle and high-dosage
114 groups (LD, MD, and HD group, 10 mice in each group). Except for the NC group, the mice
115 other groups were intraperitoneally injected with CTX at a dosage of 100 mg kg^{-1} BW (body
116 weight) once a day for 3 consecutive days to create an immunosuppressive mouse model (The
117 NC group was injected with the same dose of 0.9% normal saline solution). Afterwards,
118 lentinan, low-dose EPS, medium-dose EPS, and high-dose EPS were administered to the mice
119 by gavage at doses of 200, 100, 200, and 300 mg kg^{-1} BW once a day for 11 consecutive days.
120 The NC and MC groups were administered by gavage with an equal volume of physiological
121 saline for 11 consecutive days, and the weight of each mouse was recorded three times at one
122 time every day.

123 *2.3 Determination of delayed-type hypersensitivity (DTH) in the mice*

124 Except for the NC group, the mice in other groups were sensitized by intraperitoneal
125 injection of 0.2 mL of 2% (v/v) SRBC 24 h after the last gavage. After 4 d, the thickness of the
126 left rear toe was measured and recorded as D₁; after subcutaneously injecting 20% SRBC (20
127 μL) at the measurement site for 24 h, the thickness of the left posterior toe was measured and
128 recorded as D₂. The toe thickness difference was calculated by subtracting D₁ from D₂.

129 *2.4 Determination of phagocytic index in mouse phagocytic cells*

130 Mice were injected intravenously with 20% Indian ink (10 mL kg⁻¹ BW) into their tails 24
131 h after the last gavage. After 2 min (T₁) and 7 min (T₂), 20 μL blood from the orbital vein was
132 collected respectively, which was added to 2 mL of Na₂CO₃ solution (0.1%), and mixed evenly.
133 The absorbance of the yielding solutions at 680 nm was measured, which was recorded as A₁
134 and A₂, respectively. The carbon clearance index (K) was calculated using formula (1). The
135 phagocytic index (α) was calculated according to formula (2).

136
$$K = \frac{\lg A_1 - \lg A_2}{T_1 - T_2} \quad (1)$$

137
$$\alpha = \frac{M_{\text{mouse weight}}}{M_{\text{liver weight}} + M_{\text{spleen weight}}} \times K^{1/3} \quad (2)$$

138 *2.5 Morphological analysis of spleen, thymus, and intestinal tissues*

139 The lengths of the spleen and cecum were measured, and their morphology was recorded
140 by photographing. The thymus, duodenum, jejunum, and cecum were sliced for histological
141 observation referring to Wang's method with modifications [27]. Briefly, tissues were fixed
142 with 4% paraformaldehyde for 24 h at room temperature to maintain their original cell
143 morphology, then treated with 75% ethanol for 4 h, 90% ethanol for 2 h, 95% ethanol for 2 h,
144 and anhydrous ethanol for 1 h for gradient dehydration, followed by repeated treatments with

145 xylene 3 times for 10 min. The processed tissue samples were treated with melted paraffin
146 overnight at 65°C. Afterwards, the wax block was cut into thin slices (4 μm), laid on a glass
147 slide, and baked at 65°C. The slices were treated with xylene twice for 20 min, followed by
148 gradient hydration with anhydrous ethanol, 95%, 90%, and 75% ethanol, successively. Finally,
149 routine hematoxylin-eosin (HE) staining was used to observe the pathological changes of the
150 thymus and intestinal tissues under a microscope and photographed.

151 *2.6 Effect of EPS on immune organ indices*

152 After completion of the treatment, the mice were dissected to obtain the spleen and thymus
153 quickly, and excess tissue and fat on the surface of the organs were eliminated. After washing
154 with ice-cold PBS, the spleen and thymus were blotted with filter paper, weighed separately,
155 and recorded. The immune organ index (*I*) was calculated according to formula (3).

$$156 \quad I (\%) = \frac{M_{\text{immune organ weight}}}{M_{\text{mouse body weight}}} \times 100 \quad (3)$$

157 *2.7 Determination of spleen lymphocyte activity*

158 The separation of splenic lymphocytes was performed according to Liu's method with
159 modification [28]. Briefly, 5 mL of mouse lymphocyte separation solution was added to a 35
160 mm culture dish, which was covered with a 200-mesh nylon mesh, and then the spleen was
161 cleaned with RPMI-1640 medium and placed on the nylon mesh. The spleen was grounded
162 with a sterile pestle, and the force was controlled to ensure that the nylon mesh was suspended
163 in the separation solution without touching the bottom of the culture dish during the grinding
164 process. The separation solution containing spleen cells was then transferred to a 15 mL sterile
165 centrifuge tube and 500 μL of RPMI-1640 medium was added. After centrifugation at 800 g
166 for 5 min, the lymphocyte layer was gently aspirated into a new sterile centrifuge tube, 10 mL

167 of RPMI-1640 medium was added, washed upside down once, and centrifuged at 300 g for 10
168 min. The cells were collected and re-suspended in RPMI-1640 medium (containing 10% fetal
169 bovine serum and 1% double antibodies) evenly, and the cell density was adjusted to 3×10^6
170 cells mL⁻¹. Spleen lymphocyte suspension (100 μ L) was added to each well of the 96-well plate.
171 For the experimental group (A₁), 100 μ L of RPMI-1640 medium with Concanavalin A (final
172 concentration was 5 μ g mL⁻¹) was added; for the control group (A₂), 100 μ L of RPMI-1640
173 medium was added. The cells were incubated in a culture incubator (MCO-175, Sanyo, JAP)
174 with 5% CO₂ at 37°C for 48 h. Cell viability was determined using the MTT method, and the
175 proliferation rate of splenic lymphocytes (*R*) was calculated according to formula (4).

$$176 \quad R (\%) = \frac{A_1}{A_2} \times 100 \quad (4)$$

177 where A₁ and A₂ represent the absorbance of the experimental group and control group,
178 respectively.

179 *2.8 Determination of hemolysin and cytokines in mouse Serum*

180 Briefly, the blood taken from the orbit of mice was centrifuged at 3000 g for 10 min at
181 4°C, and the obtained serum was used for the analysis of hemolysin, IL-10, TNF- α , and IFN- γ
182 contents according to the instructions of the ELISA kits.

183 *2.9 Analysis of immunomodulatory mechanism in RAW 264.7 macrophages*

184 The TLR4 and MAPK signaling pathways are closely related to immune regulation, and
185 activation of the signaling pathway leads to iNOS release and the secretion of cytokines, such
186 as TNF- α , IL-1 β , and IL-6. Herein, the activation of TLR4 and MAPK signaling pathways was
187 verified through protein inhibitor method. Cell adhesion culture was performed on a 24-well
188 microplate. Firstly, RAW 264.7 cells in the logarithmic growth phase were collected and the

189 cell suspension was adjusted to 3×10^5 cells mL^{-1} , and cultured in a 24-well plate (1 mL per
190 well) at 37 °C for 24 h. After the cells adhered to the wall, the medium was discarded and the
191 cells were gently washed with 200 μL PBS twice. Subsequently, 100 μL of DMEM medium
192 containing different inhibitors (TLR4 inhibitor TAK-242, final concentration 10 $\mu\text{g mL}^{-1}$;
193 ERK1/2 inhibitor CI-1040, JNK1/2 inhibitor SP600125, and p38 inhibitor SB239063, final
194 concentration 20 μM) was added into the wells for 1 h treatment. Afterwards, all the groups
195 (EPS treatment group: 1 mL of DMEM medium (containing EPS with a final concentration of
196 500 $\mu\text{g mL}^{-1}$) was added; Positive control group: 1 mL DMEM medium (containing LPS with
197 a final concentration of 1 $\mu\text{g mL}^{-1}$) was added; Control group: 1 mL of DMEM medium was
198 added) were continued to incubate for 24 h. After centrifugation at 8000 rpm for 5 min, the
199 supernatant was collected and used for the measurement of the NO content using the NO assay
200 kit, and determination of the IL-1 β , IL-6, and TNF- α contents according to the ELISA kit
201 instructions.

202 *2.10 Gut microbiota analysis and intestinal SCFAs determination*

203 The DNA extraction from fecal sample and 16S rDNA sequencing were carried out at
204 Shanghai Majorbio Co. Ltd. The concentration and purity of the extracted DNA were detected
205 using a ultramicro spectrophotometer (NanoDrop2000, Thermo, USA), DNA integrity was
206 detected using agarose gel electrophoresis, 338F_806R amplification primers (388F:
207 ACTCCTACGGGAGGCAGCAG, 806R: GGACTACHVGGGTWTCTAAT) were used to
208 amplify the V3-V4 region of bacterial 16S rDNA, and the Illumina Miseq sequencing platform
209 (Illumina, San Diego, CA, USA) was used for sequencing. All analysis results were based on
210 sequencing reads and operational taxonomic units (OTUs).

211 The feces obtained from the cecum were quickly frozen with liquid nitrogen, and stored
212 at -80°C for later use. The determination of SCFAs was conducted by the reported method with
213 minor modifications [29]. Briefly, 500 mL of 4 °C pre-cooled PBS was added into frozen feces
214 and thoroughly mixed, then centrifuged at 8000 rpm for 10 min, the supernatant was evenly
215 mixed with 200 µL of crotonic acid, and kept at -20°C overnight. After centrifugation at 10000
216 rpm for 10 min at 4°C, the supernatant was filtered with 0.22 µM sterile filter membrane (water
217 system) prior to the analysis of SCFAs using gas chromatography (USA, Waters).

218 *2.11 Statistical Analysis*

219 One-way analysis of variance (ANOVA) was performed using SPSS version 25 (SPSS
220 Inc., Chicago, IL, US) to compare the results. Duncan's multiple-range test was used to analyze
221 the significance of the differences. If $P < 0.05$, the differences were considered statistically
222 significant. All the data were expressed as mean \pm standard deviation (SD).

223

224 **3. Results and Discussion**

225 *3.1 Effect of EPS on the mouse body weight*

226 Cyclophosphamide (CTX) is commonly used in the treatment of various cancers and
227 autoimmune diseases [30]. However, CTX treatment can also suppress the immune system,
228 leading to immune response inhibition [22], thus it has been widely applied to establish
229 immunosuppressive murine model [30,31]. After a successive 3-day injection with CTX, the
230 mice exhibited decreased appetite, decreased activities, and curled back, showing significant
231 differences in appearance and behavior compared to the normal control (NC) group. As shown
232 in Fig. 2, after injection with CTX, the body weight (BW) of the mice showed a gradual

233 decrease trend. This is because CTX can cause humoral immune responses, disrupting the
234 intestinal mucosal barrier, thereby disrupting gut microbiota [31,32]. Intestinal damage hinders
235 the intake of nutrients, leading to weight loss of the mice. From the 4th day, the BW of the mice
236 in EPS-treated groups began to rebound with increasing EPS dosage. At the end of treatment,
237 the BW of the high EPS dosage (HD) group increased by 18.45% compared to the MC group,
238 recovering to 95.91% of the NC group ($P>0.05$), which was higher than that in the positive
239 control (PC) group. These results indicated that EPS has an improving effect on weight loss
240 caused by CTX, which may be achieved by repairing the intestine and promoting nutrient
241 absorption. A similar result was reported for the CTX-induced immunosuppressed mice treated
242 with EPS from *Lactiplantibacillus plantarum* JLAU103 [33]. The authors posited that EPS
243 might modulate gut microbiota composition and repair the damage to the intestine induced by
244 CTX.

245 3.2 Effect of EPS on DTH and phagocytic index of mouse phagocytes

246 DTH is a type of hypersensitivity reaction mediated by T lymphocytes, which belongs to
247 cellular immunity [34]. Activation of T lymphocytes after sensitization can lead to the initiation
248 of a localized turgor response, and the extent of the local tissue swelling caused by the
249 inflammatory reaction serves as an indicator of the cellular immune activity. Phagocytes can
250 phagocytose and digest senescent and dead cells and foreign objects [35], which is an important
251 mechanism for the body's natural defense. These two indicators can reflect the state of the
252 body's immune system. As illustrated in Table 1, compared with the NC group, the toe
253 thickness was increased by 20.41% and the phagocytic index was significantly decreased in
254 the MC group ($P<0.05$). Treatments with EPS decreased the toe thickness and increased the

255 phagocytic index of the mice dose-dependently, and both the toe thickness and the phagocytic
256 index in the HD group recovered to a level close to that of the NC group ($P>0.05$), exhibiting
257 a better effect than that of the PC group. The reason for the decrease in DTH and increase in
258 phagocytic index in the presence of EPS in CTX-induced immunocompromised mice may
259 involve the regulation of cell signaling pathways, changes in immune cell activity, and
260 regulation of cytokine expression. It was reported that polysaccharides from *Radix isatidis*
261 might affect DTH by regulating the expression of immune related cytokines [33,36]. Li et al.,
262 found that polysaccharide from *G. Frundosa* protected CTX-induced immunosuppressed mice
263 through the MAPKs signaling pathway, thereby increasing phagocytic index [37].

264 3.3 Effect of EPS on the morphology of spleen, thymus, and intestine

265 As depicted in Fig. 3A, the spleen of NC mice was plump and full, while the spleen of
266 MC group showed a significant atrophy and reduction. EPS treatment tended to recover the
267 spleen morphology and size. The spleen length of HD group was closer to that of NC group
268 ($P>0.05$). Compared with NC group, the colon length in MC group was significantly shorter
269 ($P<0.05$) (Fig. 3B). EPS treatment increased the colon length of the immunosuppressed mice
270 dose-dependently. The colon length of HD group mice was significantly increased compared
271 to MC group, and recovered to the level of NC group. As shown in Fig. 3C, the boundaries
272 between the cortex and medulla of the thymus (indicated by the arrows) in the NC group were
273 found to be clear, while those in the MC group were blurred. In the EPS groups, thymus of the
274 mice recovered to varying degrees, depending on the EPS dosage. A clear boundary between
275 the thymic cortex and medulla of the mice in HD group was observed (Fig. 3C). Effects of EPS
276 on the growth of the duodenum, jejunum, ileum, and colon in immunosuppressed mice are

277 presented in Fig. 3D. The intestinal cells and villi of the MC group mice were damaged and
278 shortened, and were improved to varying degrees after treatment with EPS. In the HD group,
279 all organs were considerably recovered, with complete and neatly arranged villi (Fig. 3De),
280 indicating the marked therapeutic effect of EPS on the CTX-induced immune organ damage.
281 It is likely that polysaccharides promote the proliferation and transformation of lymphocytes,
282 induce cytokines, inhibit inflammatory responses, promote the proliferation and differentiation
283 of intestinal epithelial cells, enhance the expression of genes related to intestinal mucosal
284 integrity by modulating specific signaling pathways, thereby promoting the repair of damaged
285 immune organs and intestine [38,39].

286 *3.4 Effect of EPS on immune organ indices and spleen lymphocyte activity*

287 Thymus is the site for the development and maturation of T lymphocytes, and the spleen
288 is the largest immune organ in the human body, playing an important role in immune regulation
289 [40,41]. As shown in Table 2, both of the spleen and thymus indices of the MC group were
290 significantly lower than those of the NC group ($P<0.05$), the proliferation rate of lymphocytes
291 was also significantly decreased ($P<0.05$), indicating the CTX-induced damage of the immune
292 organs. EPS treatments improved the immune organ index and the proliferation rate of splenic
293 lymphocytes dose-dependently, and those values in the HD group even reached the level of the
294 NC group ($P>0.05$), indicating that EPS effectively improved the atrophy of immune organs
295 by promoting the proliferation and activation of immune cells. This finding is similar to that of
296 Guo et al., who found that the EPS from *Lactococcus lactis* subsp. *lactis* could defend
297 immunity organs against injury induced by CTX therapy [42].

298 *3.5 Effect of EPS on hemolysin and cytokines in mouse serum*

299 The serum hemolysin level reflects the ability of B cells to secrete specific antibodies into
300 bodily fluids after contact with characteristic antigens, thus can be used to judge the strength
301 of humoral immune function in organisms [37]. Cytokines can specifically bind to receptors on
302 the surface of target cells, causing cell proliferation, differentiation, inflammatory response and
303 immune response, and enhancing the ability of bodies to resist and eliminate the foreign
304 pathogens [43]. As shown in Table 3, the HC₅₀ (the concentration needed to cause 50%
305 hemolysis of red blood cells, represents the serum hemolysin level in mice), IFN- γ , TNF- α ,
306 and IL-10 levels in mouse serum in the MC group were all significantly lower than those in the
307 NC group ($P < 0.05$). Compared with MC group, the hemolysin and the cytokine levels in the
308 EPS treatment groups were increased dose-dependently, and these indices in the HD group
309 were closed to those of the NC group ($P > 0.05$), which were higher than those in the PC group.
310 These results indicated that EPS had a good ability to recover serum hemolysin levels and
311 promote the secretion of cytokines in the immunosuppressed mice. EPS enhanced serum
312 hemolysin and cytokine levels in CTX-induced immunosuppressed mice possibly by regulating
313 immune cell activity and improving intestinal mucosal barrier function.

314 *3.6 Immunomodulatory mechanism analysis using RAW264.7 cell model*

315 Macrophages phagocytose pathogens and cell debris, activate lymphocytes or other
316 immune cells, and respond to pathogens, thus are important barriers for the body to defend
317 against foreign objects and pathogen invasion [44]. There are abundant macrophages in the
318 intestine, which maintain and regulate the stability of the intestinal environment [45]. After
319 activation, macrophages promote the synthesis and secretion of chemokines and cytokines,
320 enhancing the immune system of the body.

321 Toll-like receptors (TLR) are a series of important proteins involved in non-specific
322 immunity, widely distributed on the surface of various cells in the immune system, mediating
323 pathogen related molecular pattern recognition [46], and serving as a bridge connecting non-
324 specific and specific immunities. Mitogen-activated protein kinases (MAPKs) are a group of
325 serine/threonine protein kinases that can be activated by numerous external stimuli and play an
326 important role in signal transduction, participating in numerous important physiological
327 activities, such as cell proliferation, differentiation, inflammation, and apoptosis. MAPKs
328 mainly include p38 mitogen-activated protein kinase (p38), extracellular regulated kinase
329 (ERK), and c-Jun N-terminal kinase (JNK) [47]. The MAPK signaling pathway in RAW 264.7
330 cells can be activated by LPS, and the activated MAPK family proteins can activate NF- κ B
331 inhibitor, which causes the release of NF- κ B and subsequent transfer to the nucleus, inducing
332 transcription of immune-related genes and activating RAW 264.7 immune response.

333 In our previous work, EPS was found to activate the NF- κ B signaling pathway, and
334 promote the release of NO and secretion of TNF- α , IL-1 β and IL-6 by upregulating the
335 expression of mRNA encoding iNOS and the corresponding cytokines [25]. The activation of
336 NF- κ B can be achieved through various pathways, including the TLR4 signaling pathway [48].
337 In addition, MAPK signaling pathway can affect the activation of NF- κ B. For example,
338 activation of p38 MAPK can lead to phosphorylation of I κ -B, thereby promoting activation
339 and nuclear translocation of NF- κ B; the activation of NF- κ B can also in turn affect the activity
340 of the MAPK pathway, forming a complex regulatory network [47]. In this study, to further
341 clarify whether TLR4 and MAPK signaling pathways were involved in EPS-induced immune
342 activation in RAW 264.7 macrophages, TLR4 specific inhibitor TAK-242, ERK1/2 inhibitor

343 (CI-1040), JNK1/2 inhibitor (SP600125), and p38 inhibitor (SB239063) were used to examine
344 the release of NO, TNF- α , IL-1 β and IL-6 by EPS-treated RAW 264.7 cells. As shown in Fig.
345 4A, addition of TLR4 specific inhibitor TAK-242 in the NC group had no significant difference
346 in the secretion of NO, TNF- α , IL-1 β , and IL-6 ($P>0.05$). In the EPS or lipopolysaccharide
347 (LPS)-stimulated RAW 264.7 cells, the NO, TNF- α , IL-1 β , and IL-6 levels showed a significant
348 increase when compared to the NC group ($P<0.05$), indicating the activation of immune
349 response, while addition of inhibitors significantly decreased the secretion of NO, TNF- α , IL-
350 1 β , and IL-6 by RAW 264.7 ($P<0.05$), indicating that TAK-242 specifically bound to TLR4,
351 blocking the binding of EPS or LPS to TLR4, which led to a decrease in the immune activation.
352 Polysaccharides from multiple sources have been proven to regulate immunity by activating
353 the TLR4 signaling pathway. Liu et al. also had the same results when studying the
354 immunostimulatory effect of polysaccharides [47]. Tian et al. verified that polysaccharides
355 from *Poria Cocos* exert immune regulatory effects through the TLR4 signaling pathway using
356 TLR4 deficient mouse model [49].

357 As presented in Fig. 4B, addition of ERK1/2, JNK1/2 and p38 inhibitors in RAW 264.7
358 cells (NC group) did not affect the release of NO, TNF- α , IL-1 β , and IL-6, indicating that the
359 inhibitors did not induce the immune response in RAW 264.7 cells. In the EPS-induced group,
360 the release of NO, TNF- α , IL-1 β , and IL-6 showed a significant increase compared to the NC
361 group, while the addition of inhibitors significantly decreased the release of NO, TNF- α , IL-
362 1 β , and IL-6 ($P<0.05$), indicating that specific inhibition of the three subunits of MAPKs can
363 block the MAPK signaling pathway, confirming the involvement of the MAPK signaling
364 pathway in immune response of EPS-activated RAW 264.7 cells. This finding agrees with that

365 of Wei et al., who reported that addition of MAPK inhibitors decreased the production of NO,
366 IL-6, and TNF- α in *Astragalus* polysaccharide RAP-stimulated RAW 264.7 cells [50].

367 3.7 Effect of EPS on the gut microbiota of mice

368 3.7.1 Analysis of microbial richness, Venn diagram and α -diversity

369 The Shannon Wiener dilution curve (Fig. 5Aa) showed that as the sequencing amount
370 increases, the curve tended to be flat, indicating that all samples for this sequencing have
371 sufficient data volume. The Rank Abundance curve (Fig. 5Ab) of the gut microbiota in the MC
372 group had a shorter span and lower smoothness compared to other groups, indicating the lower
373 richness and evenness of microbiota. The curve of the HD group showed a significant
374 improvement in span and smoothness, being close to the NC group, which indicated that EPS
375 restored the abundance and uniformity of the intestinal microbiota in immunosuppressed mice.
376 The Venn diagram (Fig. 5B) showed the overlap between these sets of groups, there were 5
377 unique OTUs in the MC group, 10 in the HD group, 6 in the PC group, and 4 in the NC group.
378 From the shared OTU data, there were 510 overlapping OTUs in the four samples, the
379 overlapping number of OTUs in the MC, HD and PC groups with NC group was 544, 567 and
380 566, respectively. Therefore, treatment with EPS can increase the number of OTUs in the
381 intestine of immunosuppressive mice and increase their similarity with the NC group. Wan et
382 al. had similar findings in exploring the effect of EPS from *Lactobacillus rhamnosus* ZFM231
383 on gut microbiota in DSS-induced colitis mice [51].

384 The α -diversity refers to the diversity or richness of species in a specific ecosystem or
385 community. As shown in Fig. 5C, compared to the NC group, the Ace index (Fig. 5Ca) and
386 Chao index (Fig. 5Cb) in the MC group were significantly reduced, indicating a decrease in

387 the number of gut microbiota. The significant decrease in both richness and diversity in the
388 intestinal microbiota of immunosuppressed mice is attributed to the CTX-induced intestinal
389 damage, changes in immune ability, metabolic change or direct effects of CTX on the intestinal
390 microbiota environment. After the EPS treatment, the Ace and Chao indices of the HD group
391 increased significantly, reaching the level of the NC group ($P>0.05$). Compared with NC group,
392 the Shannon Wiener index (Fig. 5Cc) in the MC group showed a significant decrease ($P<0.05$),
393 while the Simpson index (Fig. 5Cd) showed a significant increase, which indicated a decrease
394 in gut microbiota diversity. In the HD group, the Shannon Wiener index significantly increased
395 ($P<0.05$), while the Simpson index significantly decreased ($P<0.05$). Therefore, EPS
396 effectively enhanced the diversity and richness of gut microbiota in the mice. This result agrees
397 with that of Zhu et al. [52].

398 3.7.2 Analysis of microbial community structure

399 The structural composition of mouse gut microbiota was analyzed at the phylum and
400 family levels (Fig. 6). At the phylum level (Fig. 6A), Bacteroidota and Firmicutes were the
401 dominant phyla, accounting for approximately 96% of the total bacterial count. This result is
402 consistent with that of a previous report, in which over 90% of bacteria in the intestine lumen
403 pertain to the phyla Firmicutes and Bacteroidetes [53]. Firmicutes and Bacteroidetes are
404 capable of encoding various carbohydrate-active enzymes and are important for the utilization
405 of nondigestible polysaccharides [54]. Compared to the NC group, the Bacteroidota level in
406 the MC group was significantly increased ($P<0.05$), while the Firmicutes level was
407 significantly reduced ($P<0.05$). In the HD group, the Bacteroidota level was significantly
408 decreased ($P<0.05$), and the Firmicutes level was significantly increased ($P<0.05$) compared

409 with MC group. The Firmicutes/Bacteroidetes (F/B) ratio in the HD group had no statistical
410 difference with the NC group ($P>0.05$), indicating an effective regulation of high dosage EPS
411 on the intestinal flora structure at phylum level. Previous reports have shown that a higher F/B
412 ratio indicates an elevated capability of intestinal flora to absorb calories from the diet [55],
413 which also explain why EPS can restore body weight in immunosuppressed mice in this study.

414 Analysis at the family level (Fig. 6B) indicated that *Muribacoccaceae*, *Lachnospiraceae*,
415 and *Prevotellaceae* were the dominant bacterial families, accounting for about 75% of the total
416 bacteria. Compared with the NC group, the *Muriaculaceae* and *Prevotellinaceae* in the MC
417 group significantly increased ($P<0.05$), while the abundance of *Lachnospiraceae*,
418 *Oscillospiraceae*, *norank_o_Clostridia_UCG-014*, *Rikenellaceae*, *Ruminococcaceae* and
419 *Bacteroidaceae* significantly decreased ($P<0.05$). In the HD group, *Muribacoccaceae* and
420 *Prevotellaceae* significantly decreased ($P<0.05$), *Lachnospiraceae*, *Oscillospiraceae*,
421 *norank_o_Clostridia_UCG-014*, *Ruminococcaceae* and *Bacteroidaceae* significantly increased
422 ($P<0.05$), when compared to the MC group; the composition of the bacterial community was
423 also closer to the NC group. The above results suggest that EPS could modulate the gut
424 microbiota in the immunosuppressive mice, recovering the microbiota to the normal level.

425 3.7.3 Analysis of β -diversity

426 β -Diversity analysis is generally used to analyze the differences in species diversity
427 between different communities or samples under different conditions [56]. As depicted in Fig.
428 7A, the colors of the intersection areas between the MC and HD groups, the PC and NC groups
429 were generally darker, indicating that there were significant differences in the species
430 composition. However, the color of the intersection areas between the HD, PC, and NC groups

431 was generally lighter, indicating that the similar differences in distance values. This further
432 demonstrated that EPS effectively improved the intestinal microbiota disorder caused by CTX
433 in the mice, restoring the microbiota structure to normal levels.

434 Principal coordinate analysis (PCoA) is an unconstrained data dimensionality reduction
435 method that can be used to study the similarity or dissimilarity of sample community
436 compositions. As presented in Fig. 7B, the MC group was significantly separated from other
437 groups, indicating the significant differences in the composition of the gut microbiota. In the
438 HD group, the composition of gut microbiota changed, and the overlapping areas also increased,
439 being closer to the NC group, which indicated that EPS effectively recovered the gut microbiota
440 in the immunosuppressive mice.

441 3.7.4 Analysis of LEfSe

442 LEfSe analysis is mainly used to identify the species that best represent the differences
443 between two or more groups of samples. Significant differences in species at the phylum and
444 family levels were compared through LEfSe analysis between the MC and NC groups, between
445 the MC and HD groups, between the HD and NC groups, and between the HD and PC groups
446 (Fig. 8A). There were 9 different species between the MC and NC groups, among which f_
447 *Muribaculaceae* and f_*Erysipelotrichaceae* were in the MC group, other 7 species were in
448 the NC group, the top 5 being o_*Oscillospirales*, f_*Rumnococcaceae*, f_
449 *Hungateiclosridiaceae*, f_*Anaerovoracaceae* and o_*RF39*. There were 14 different species
450 between MC and HD groups, of which 2 were in MC group, namely o_*Erysipelotrichales*,
451 f_*Erysipelotrichaceae*, and 12 were in the HD group, and the top 5 being o_*Oscillospirales*,
452 f_*Rumnococcaceae*, o_*Sphingomonadales*, f_*Sphingomonadaceae*, f_

453 *Hungateiclostridiaceae*. Based on the differences in microbial communities between the two
454 comparative groups, the significant differences in species *f_Muribaculaceae*,
455 *o_Erysipelotrichales*, and *f_Erysipelotirichaceae* in the MC group may be closely related to
456 the imbalance of gut microbiota. This finding is similar to that of Chung et al. [57]. EPS
457 treatment significantly changed the abundance of *o_Oscillospirales*, *f_Rumnococcaceae*, and
458 *f_Hungateichostridiaceae*, and these species might play an important role in regulating the gut
459 microbiota. In addition, more differential microbiota was found in the HD group, which might
460 be related to the increase in the abundance of some gut microbiota.

461 *3.8 Effect of EPS on SCFA production and analysis of environmental factors associated with* 462 *gut microbiota*

463 SCFAs are the main metabolic products produced by the external ingestion or
464 decomposition of carbohydrates by gut microbiota, including acetic acid, propionic acid,
465 isobutyric acid, butyric acid, isovaleric acid, and valeric acid. SCFAs can maintain the pH in
466 the intestine and are absorbed and utilized as the main energy substance in the intestine [58,59].
467 As shown in Fig. 8A, the contents of acetic acid, propionic acid, butyric acid, and valeric acid
468 in the MC group mice were significantly lower than those in the NC group ($P<0.05$), while no
469 significant difference in the contents of isobutyric acid and isovaleric acid in different groups
470 was observed ($P>0.05$). EPS intervention resulted in a dose-dependent increase in the levels of
471 acetic acid, propionic acid, butyric acid, and valeric acid. In the HD group, the levels of the
472 above SCFAs approached those of the NC group. The majority of polysaccharides are difficult
473 to be digested or absorbed in the small intestine, due to the limited number of genes encoding
474 carbohydrate-active enzymes in mammalian bodies [60]. In the intestinal tract of mice, EPS

475 was decomposed by numerous microorganisms, producing the SCFAs. The absorbed SCFAs
476 might participate in the immune regulation, promoting the recovery of immunity of the
477 immunosuppressed mice. Overall, EPS has good regulatory and restorative effects on the SCFA
478 level in the intestine of immunosuppressed mice.

479 As presented in Fig. 8B, the redundancy analysis (RDA) showed the correlation between
480 the intestinal species and propionic acid, isobutyric acid, and isovaleric acid was relatively
481 small, while there was a significant correlation between intestinal species and acetic acid,
482 butyric acid, and valeric acid. Species showing a significant positive correlation include:
483 *Clostridium_methylpentosum_group*, *Ruminococcaceae*, *Anaerovoracaceae*,
484 *Christensenellaceae*, *Hungateiclostridicaceae*, *Prevotellaceae*, etc. Based on the analysis of
485 species differences between groups, it was found that the above species included some
486 significantly different species in the HD group, indicating that EPS could be metabolized by
487 the above species to produce SCFAs such as acetic acid, butyric acid, and valeric acid, thereby
488 altering the intestinal microenvironment and affecting the structure of the intestinal microbiota.
489 A variety of gut microbiota can utilize polysaccharides, which are metabolized into small
490 molecules such as SCFAs in the intestine. Such small molecules are more conducive to
491 absorption, and they can also directly stimulate the immune cells of the body to induce an
492 immune response, thereby promoting immune enhancement.

493 3.9 Prediction and analysis of microbial association function

494 The classification and functional proportion of COG (Clusters of Orthologous Groups)
495 prediction functions in the gut microbiota are shown in Fig. 8C. A total of 21 predicted
496 functional pathways were obtained, among which the more abundant functions include

497 'translation, ribosomal structure and biogenesis', 'amino acid transport and metabolism',
498 'carbohydrate transport and metabolism, transcription', and 'cell wall/membrane/envelope
499 biogenesis'. These functions are all closely related to life activities, and it can be concluded
500 that the gut microbiota plays a crucial role in various life activities of the human body. Analysis
501 of the effect of EPS on the functional pathways of immunosuppressed mice indicated that all
502 19 functional pathways were enhanced in the HD group, with the most significant five
503 functions being: 'cytoskeleton', 'cell motility', 'transcription', 'signal transduction
504 mechanisms', and 'replication, recombination, and repair'. These functions are closely related
505 to the repair of tissue damage caused by CTX, promotion of cytokine production, and activation
506 of signaling pathways, further revealing the immunoregulatory mechanism of EPS by
507 influencing the gut microbiota in immunosuppressive mice.

508

509 **4. Conclusion**

510 In this work, EPS produced by *L. rhamnosus* ZFM216, grew in a newly developed culture
511 medium, was demonstrated to possess a considerable immune-regulatory effect using a CTX-
512 induced immunosuppressive mouse model. The immunomodulatory mechanism of this EPS
513 was systematically investigated for the first time at cells and animal levels. It can be concluded
514 that TLR4/MAPK/NF- κ B signaling pathways are involved in the immune regulation of EPS.
515 EPS could also effectively restore the richness and diversity of gut microbiota.
516 *Clostridium_methylpentosum_Group*, *Ruminococcaceae*, *Anaerovoracaceae*,
517 *Christensenellaceae*, *Hungateiclostridicaceae*, *Prevotellaceae*, etc. were positively correlated
518 with the production of acetic acid, butyric acid, and valeric acid, which alter the intestinal

519 microenvironment and affect the structure of intestinal microbiota, and consequently
520 stimulating the immune cells and exerting immuno-enhancing effects. EPS developed in the
521 present study has promising application as an ingredient of functional foods due to its potent
522 immunomodulatory effect. However, evaluations of the long-term effects and more extensive
523 safety of the EPS are still required in the future.

524 **Acknowledgements**

525 This work was supported by "Pioneer" and "Leading Goose" R&D Program of Zhejiang
526 (2022C02012), and A Project Supported by Scientific Research Fund of Zhejiang Provincial
527 Education Department (Y202353416).

528 **Declaration of interest**

529 The authors declare that they have no known competing financial interests or personal
530 relationships that could have appeared to influence the work reported in this paper.

531 **Author Contributions**

532 L.C.: Investigation, Writing-Original draft preparation. D.W.: Methodology, Investigation.
533 W.L.: Supervision. S.Z.: Writing-Review & Editing. Q.G.: Resource, Supervision. T.Z.:
534 Conceptualization, Supervision, Funding acquisition, Writing-Review & Editing.

535 **References**

- 536 [1] C. Li, Y. Ma, Z. Mi, R. Huo, T. Zhou, H. Hai, L.Y. Kwok, Z. Sun, Y. Chen, H. Zhang, Screening for
537 *Lactobacillus plantarum* strains that possess organophosphorus pesticide-degrading activity and
538 metabolomic analysis of phorate degradation, *Front. Microbiol.* 9 (2018) 2048.
539 <https://doi.org/10.3389/fmicb.2018.02048>
- 540 [2] L. Wang, H. M. Liu and G. Y. Qin, Structure characterization and antioxidant activity of
541 polysaccharides from Chinese quince seed meal, *Food Chem.* 234 (2017) 314–322.
542 <https://doi.org/10.1016/j.foodchem.2017.05.002>

- 543 [3] M. Kwon, J. Lee, S. Park, O.-H. Kwon, J. Seo, S. Roh, Exopolysaccharide isolated from *Lactobacillus*
544 *plantarum* L-14 has anti-inflammatory effects via the toll-like receptor 4 pathway in LPS-induced
545 RAW 264.7 Cells, *Int. J. Mol. Sci.* 21 (2020) 9283. <https://doi.org/10.3390/ijms21239283>
- 546 [4] A. Hussain, K.M. Zia, S. Tabasum, A. Noreen, M. Ali, R. Iqbal, M. Zuber, Blends and composites of
547 exopolysaccharides; properties and applications: A review, *Int. J. Biol. Macromol.* 94 (2017) 10–27.
548 <https://doi.org/10.1016/j.ijbiomac.2016.09.104>
- 549 [5] T. Aziz, H. Xingyu, A. Sarwar, M. Naveed, M.A. Shabbir, A.A. Khan, T. Ulhaq, M. Shahzad, Y.
550 Zhennai, A. Shami, M.Y. Sameeh, S.A. Alshareef, M.A. Tashkandi, R.S. Jalal, Assessing the probiotic
551 potential, antioxidant, and antibacterial activities of oat and soy milk fermented with
552 *Lactiplantibacillus plantarum* strains isolated from Tibetan Kefir, *Front. Microbiol.* 14 (2023)
553 1265188. <https://doi.org/10.3389/fmicb.2023.1265188>
- 554 [6] J. Wang, T. Wu, X. Fang, W. Min, Z. Yang, Characterization and immunomodulatory activity of an
555 exopolysaccharide produced by *Lactobacillus plantarum* JLK0142 isolated from fermented dairy tofu,
556 *Int. J. Biol. Macromol.* 115 (2018) 985–993. <https://doi.org/10.1016/j.ijbiomac.2018.04.099>
- 557 [7] C. Ma, H. Guo, H. Chang, S. Huang, S. Jiang, D. Huo, J. Zhang, X. Zhu, The effects of
558 exopolysaccharides and exopolysaccharide-producing *Lactobacillus* on the intestinal microbiome of
559 zebrafish (*Danio rerio*), *BMC Microbiol.* 20 (2020) 300. <https://doi.org/10.1186/s12866-020-01990-6>
- 560 [8] Q. Wang, J. Shao, L. Shen, J. Xiu, S. Shan, K. Ma, Pretreatment of straw using filamentous fungi
561 improves the remediation effect of straw biochar on bivalent cadmium contaminated soil, *Environ. Sci.*
562 *Pollut. Res.* 29 (2022) 60933–60944. <https://doi.org/10.1007/s11356-022-20177-2>
- 563 [9] T. Aziz, M. Naveed, A. Sarwar, S.I. Makhdoom, M.S. Mughal, U. Ali, Z. Yang, M. Shahzad, M.Y.
564 Sameeh, M.W. Alruways, A.S. Dablood, A.A. Almalki, A.S. Alamri, M. Alhomrani, Functional
565 annotation of *Lactiplantibacillus plantarum* 13-3 as a potential starter probiotic involved in the food
566 safety of fermented products, *Molecules* 27 (2022) 5399. <https://doi.org/10.3390/molecules27175399>
- 567 [10] J. Wu, H. Gao, W. Ge, J. He, Over expression of PTEN induces apoptosis and prevents cell
568 proliferation in breast cancer cells, *Acta. Biochim. Pol.* 67 (2020) 515-519.
569 https://doi.org/10.18388/abp.2020_5371
- 570 [11] W. Wang, X. Li, D. Li, F. Pan, X. Fang, W. Peng, W. Tian, Effects of major royal jelly proteins on the
571 immune response and gut microbiota composition in cyclophosphamide-treated mice, *Nutrients* 15
572 (2023) 974. <https://doi.org/10.3390/nu15040974>

- 573 [12] M. Zhang, X.N. Hao, T. Aziz, J. Zhang, Z.N. Yang, Exopolysaccharides from *Lactobacillus plantarum*
574 YW11 improve immune response and ameliorate inflammatory bowel disease symptoms, *Acta.*
575 *Biochim. Pol.* 67 (2020) 485-493. https://doi.org/10.18388/abp.2020_5171
- 576 [13] M. Claus, N. Dychus, M. Ebel, J. Damaschke, V. Maydych, O.T. Wolf, T. Kleinsorge, C. Watzl,
577 Measuring the immune system: a comprehensive approach for the analysis of immune functions in
578 humans, *Arch. Toxicol.* 90 (2016) 2481–2495. <https://doi.org/10.1007/s00204-016-1809-5>
- 579 [14] X. Pan, C. Li, J. Feng, The role of LncRNAs in tumor immunotherapy, *Cancer Cell Int.* 23 (2023) 30.
580 <https://doi.org/10.1186/s12935-023-02872-3>
- 581 [15] D. Usharauli, Chronic infection and the origin of adaptive immune system, *Med. Hypotheses* 75 (2010)
582 241–243. <https://doi.org/10.1016/j.mehy.2010.02.031>
- 583 [16] W. Zhang, W. Ma, J. Zhang, X. Song, W. Sun, Y. Fan, The immunoregulatory activities of astragalus
584 polysaccharide liposome on macrophages and dendritic cells, *Int. J. Biol. Macromol.* 105 (2017) 852–
585 861. <https://doi.org/10.1016/j.ijbiomac.2017.07.108>
- 586 [17] T. Aziz, A.A. Khan, A. Tzora, C. Voidarou, I. Skoufos, Dietary implications of the bidirectional
587 relationship between the gut microflora and inflammatory diseases with special emphasis on irritable
588 bowel disease: current and future perspective, *Nutrients* 15 (2023) 2956.
589 <https://doi.org/10.3390/nu15132956>
- 590 [18] C. Ting, V. Bansal, I. Batal, M. Mounayar, L. Chabtini, G. El Akiki, J. Azzi, Impairment of immune
591 systems in diabetes, *Adv. Exp. Med. Biol.* 771 (2013) 62–75.
- 592 [19] M. Droste, B.K. Thakur, B.P. Eliceiri, Tumor-derived extracellular vesicles and the immune system—
593 lessons from immune-competent mouse-tumor models, *Front. Immunol.* 11 (2020) 606859.
594 <https://doi.org/10.3389/fimmu.2020.606859>
- 595 [20] E. Márquez, C. Chung, R. Marches, R. Rossi, D. Nehar-Belaid, A. Eroglu, D. Mellert, G. Kuchel, J.
596 Banchereau, D. Ucar, Sexual-dimorphism in human immune system aging, *Nat. Commun.* 11 (2020)
597 751. <https://doi.org/10.1038/s41467-020-14396-9>
- 598 [21] T. Williams, M. McKenna, Exercise limitation following transplantation, *Compr. Physiol.* 2 (2012)
599 1937–1979. <https://doi.org/10.1002/cphy.c110021>
- 600 [22] G. Cai, Y. Wu, A. Wusiman, P. Gu, N. Mao, S. Xu, T. Zhu, Z. Feng, Z. Liu, D. Wang, Alhagi honey
601 polysaccharides attenuate intestinal injury and immune suppression in cyclophosphamide-induced
602 mice, *Food Funct.* 12 (2021) 6863–6877. <https://doi.org/10.1039/d1fo01008e>

- 603 [23] R. Huang, J. Xie, X. Liu, M. Shen, Sulfated modification enhances the modulatory effect of yam
604 polysaccharide on gut microbiota in cyclophosphamide-treated mice, *Food Res. 580 Int.* 145 (2021)
605 110393. <https://doi.org/10.1016/j.foodres.2021.110393>
- 606 [24] J. Wu, C. Yu, S. Shen, Y. Ren, H. Cheng, H. Xiao, D. Liu, S. Chen, X. Ye, J. Chen, RGI-type pectic
607 polysaccharides modulate gut microbiota in a molecular weight-dependent manner *In Vitro*, *J. Agric.*
608 *Food Chem.* 71 (2023) 2160–2172. <https://doi.org/10.1021/acs.jafc.2c07675>
- 609 [25] L. Chen, Q. Gu, T. Zhou, Statistical optimization of novel medium to maximize the yield of
610 exopolysaccharide from *Lacticaseibacillus rhamnosus* ZFM216 and its immunomodulatory activity,
611 *Front. Nutr.* 9 (2022) 924495. <https://doi.org/10.3389/fnut.2022.924495>
- 612 [26] Q. Xu, M.M. Wang, X.Y. Li, Y.R. Ding, X.Y. Wei, T. Zhou, Antioxidant and anti-inflammatory
613 activities and action mechanisms of exopolysaccharides from *Lactiplantibacillus plantarum* Z-1. *Food*
614 *Biosci.* 62 (2024) 105247. <https://doi.org/10.1016/j.fbio.2024.105247>
- 615 [27] Y. Wang, Y. Wu, B. Liu, H. Yang, H. Qian, Y. Cheng, X. Li, G. Yang, X. Zheng, F. Shen, Binding
616 domain peptide ameliorates alveolar hypercoagulation and fibrinolytic inhibition in mice with
617 lipopolysaccharide-induced acute respiratory distress syndrome Via NF- κ B signaling pathway, *Am. J.*
618 *Transl. Res.* 14 (2022) 3854–3863.
- 619 [28] Y. Liu, J. Cai, W. Liu, Y. Lin, L. Guo, X. Liu, Z. Qin, C. Xu, Y. Zhang, X. Su, K. Deng, G. Yan, J.
620 Liang, Intravenous injection of the oncolytic virus M1 awakens antitumor T cells and overcomes
621 resistance to checkpoint blockade, *Cell Death. Dis.* 11 (2020) 1062. [https://doi.org/10.1038/s41419-](https://doi.org/10.1038/s41419-020-03285-0)
622 [020-03285-0](https://doi.org/10.1038/s41419-020-03285-0)
- 623 [29] A. Su, G. Ma, M. Xie, Y. Ji, X. Li, L. Zhao, Q. Hu, Characteristic of polysaccharides from *Flammulina*
624 *velutipes* *in vitro* digestion under salivary, simulated gastric and small intestinal conditions and
625 fermentation by human gut microbiota, *Int. J. Food Sci. Technol.* 54 (2019) 2277–2287.
626 <https://doi.org/10.1111/ijfs.14142>
- 627 [30] A. Verma, R. Mathur, A. Farooque, V. Kaul, S. Gupta, B.S. Dwarakanath, T-Regulatory cells in tumor
628 progression and therapy, *Cancer Manag. Res.* 11 (2019) 10731–10747.
629 <https://doi.org/10.2147/CMAR.S228887>
- 630 [31] Y. Liu, X. Wu, Y. Wang, W. Jin, Y. Guo, The immunoenhancement effects of starfish *Asterias rollestoni*
631 polysaccharides in macrophages and cyclophosphamide-induced immunosuppression mouse models,
632 *Food Funct.* 11 (2020) 10700–10708. <https://doi.org/10.1039/d0fo01488e>

- 633 [32] M. Ying, B. Zheng, Q. Yu, K. Hou, H. Wang, M. Zhao, Y. Chen, J. Xie, S. Nie, M. Xie, *Ganoderma*
634 *atrum* polysaccharide ameliorates intestinal mucosal dysfunction associated with autophagy in
635 immunosuppressed mice, *Food Chem. Toxicol.* 138 (2020) 111244.
636 <https://doi.org/10.1016/j.fct.2020.111244>
- 637 [33] J. Wang, M. Li, Y. Gao, H. Li, L. Fang, C. Liu, X. Liu, W. Min, Effects of exopolysaccharides from
638 *Lactiplantibacillus plantarum* JLAU103 on intestinal immune response, oxidative stress, and
639 microbial communities in cyclophosphamide-induced immunosuppressed mice, *J. Agric. Food Chem.*
640 70 (2022) 2197–2210. <https://doi.org/10.1021/acs.jafc.1c06502>
- 641 [34] I. Roger, P. Montero, A. García, J. Milara, P. Ribera, J.A. Pérez-Fidalgo, J. Cortijo, Evaluation of
642 antineoplastic delayed-type hypersensitivity skin reactions *in vitro*, *Pharmaceuticals (Basel)*15 (2022)
643 1111. <https://doi.org/10.3390/ph15091111>
- 644 [35] B. Ginley, T. Emmons, B. Lutnick, C. Urban, B. Segal, P. Sarder, Computational detection and
645 quantification of human and mouse neutrophil extracellular traps in flow cytometry and confocal
646 microscopy, *Sci. Rep.* 7 (2017) 17755. <https://doi.org/10.1038/s41598-017-18099-y>
- 647 [36] Y. Zhao, J. Wang, L. Shan, C. Jin, L. Ma, X. Xiao, Effect of *Radix Isatidis* polysaccharides on
648 immunological function and expression of immune related cytokines in mice, *Chin. J. Integr. Med.* 14
649 (2008) 207–211. <https://doi.org/10.1007/s11655-008-0207-2>
- 650 [37] Q. Li, G. Chen, H. Chen, W. Zhang, Y. Ding, P. Yu, T. Zhao, G. Mao, W. Feng, L. Yang, X. Wu, Se-
651 enriched *G. frondosa* polysaccharide protects against immunosuppression in cyclophosphamide-
652 induced mice via MAPKs signal transduction pathway, *Carbohydr. Polym.* 196 (2018) 445–456.
653 <https://doi.org/10.1016/j.carbpol.2018.05.046>
- 654 [38] X. Kong, W. Duan, D. Li, X. Tang, Z. Duan, Effects of polysaccharides from *auricularia auricula* on
655 the immuno-stimulatory activity and gut microbiota in immunosuppressed mice induced by
656 cyclophosphamide, *Front. Immunol.* 11 (2020) 595700. <https://doi.org/10.3389/fimmu.2020.595700>
- 657 [39] X. Chen, W. Sun, B. Xu, E. Wu, Y. Cui, K. Hao, G. Zhang, C. Zhou, Y. Xu, J. Li, H. Si, Polysaccharides
658 from the Roots of *Millettia Speciosa Champ* modulate gut health and ameliorate cyclophosphamide-
659 induced intestinal injury and immunosuppression, *Front. Immunol.* 12 (2021) 766296.
660 <https://doi.org/10.3389/fimmu.2021.766296>
- 661 [40] H. Wang, W. Pan, L. Zheng, X. Zhong, L. Tan, Z. Liang, J. He, P. Feng, Y. Zhao and Y. Qiu, Thymic
662 epithelial cells contribute to thymopoiesis and T cell development, *Front. Immunol.* 10 (2020) 3099.

663 <https://doi.org/10.3389/fimmu.2019.03099>

664 [41] S. Lewis, A. Williams, S. Eisenbarth, Structure and function of the immune system in the spleen, *Sci.*
665 *Immunol.* 4 (2019) eaau6085. <https://doi.org/10.1126/sciimmunol.aau6085>

666 [42] Y. Guo, D. Pan, H. Li, Y. Sun, X. Zeng, B. Yan, Antioxidant and immunomodulatory activity of
667 selenium exopolysaccharide produced by *Lactococcus lactis* subsp. *lactis*, *Food Chem.* 138 (2013)
668 84–89. <https://doi.org/10.1016/j.foodchem.2012.10.029>

669 [43] L. Yang, T. Lu, C. Hsieh, W. Lin, Characterization and immunomodulatory activity of polysaccharides
670 derived from *Dendrobium tosaense*, *Carbohydr. Polym.* 111 (2014) 856–863.
671 <https://doi.org/10.1016/j.carbpol.2014.05.007>

672 [44] C. Liu, J. Chen, L. Chen, X. Huang, P. Cheung, Immunomodulatory activity of polysaccharide-protein
673 complex from the mushroom sclerotia of *Polyporus rhinocerus* in murine macrophages, *J. Agric. Food*
674 *Chem.* 64 (2016) 3206–3214. <https://doi.org/10.1021/acs.jafc.6b00932>

675 [45] M. Delfini, N. Stakenborg, M.F. Viola, G. Boeckxstaens, Macrophages in the gut: Masters in
676 multitasking, *Immunity* 55 (2022) 1530–1548. <https://doi.org/10.1016/j.immuni.2022.08.005>

677 [46] Q. Yu, S. Nie, J. Wang, P. Yin, D. Huang, W. Li, M. Xie, Toll-like receptor 4-mediated ROS signaling
678 pathway involved in *Ganoderma atrum* polysaccharide-induced tumor necrosis factor- α secretion
679 during macrophage activation, *Food Chem. Toxicol.* 66 (2014) 14–22.
680 <https://doi.org/10.1016/j.fct.2014.01.018>

681 [47] Y. Liu, J. Hou, M. Zhang, E. Seleh-Zo, J. Wang, B. Cao, X. An, circ-016910 sponges miR-574-5p to
682 regulate cell physiology and milk synthesis via MAPK and PI3K/AKT–mTOR pathways in GMECs,
683 *J. Cell. Physiol.* 235 (2020) 4198–4216. <https://doi.org/10.1002/jcp.29370>

684 [48] A. Stierschneider, C. Wiesner, Shedding light on the molecular and regulatory mechanisms of TLR4
685 signaling in endothelial cells under physiological and inflamed conditions, *Front. Immunol.* 14 (2023)
686 1264889. <https://doi.org/10.3389/fimmu.2023.1264889>

687 [49] H. Tian, Z. Liu, Y. Pu, Y. Bao, Immunomodulatory effects exerted by *Poria Cocos* polysaccharides via
688 TLR4/TRAF6/NF- κ B signaling in vitro and in vivo, *Biomed. Pharmacother.* 112 (2019) 108709.
689 <https://doi.org/10.1016/j.biopha.2019.108709>

690 [50] W. Wei, H. Xiao, W. Bao, D. Ma, C. Leung, X. Han, C. Ko, C. Lau, C. Wong, K. Fung, P. Leung, Z.
691 Bian, Q. Han, TLR-4 may mediate signaling pathways of *Astragalus* polysaccharide RAP induced
692 cytokine expression of RAW264.7 cells, *J. Ethnopharmacol.* 179 (2016) 243–252.

- 693 <https://doi.org/10.1016/j.jep.2015.12.060>
- 694 [51] C. Wan, W. Qian, W. Liu, X. Pi, M. Tang, X. Wang, Q. Gu, P. Li, T. Zhou, Exopolysaccharide from
695 *Lactobacillus rhamnosus* ZFM231 alleviates DSS -induced colitis in mice by regulating gut microbiota,
696 J. Sci. Food Agric. 102 (2022) 7087-7097. <https://doi.org/10.1002/jsfa.12070>
- 697 [52] Y.Z. Zhu, D. Wang, S.B. Zhou, T. Zhou, Hypoglycemic effects of *Gynura divaricata* (L.) DC
698 polysaccharide and action mechanisms *via* modulation of gut microbiota in diabetic mice, J. Agri.
699 Food Chem. 72 (2024) 9893-9905. <https://doi.org/10.1021/acs.jafc.4c00626>
- 700 [53] Y. Chen, L. Xiao, M. Zhou, H. Zhang, The microbiota: a crucial mediator in gut homeostasis and
701 colonization resistance, Front. Microbiol. 15 (2024) 1417864.
702 <https://doi.org/10.3389/fmicb.2024.1417864>
- 703 [54] P. Lapébie, V. Lombard, E. Drula, N. Terrapon, B. Henrissat, Bacteroidetes use thousands of enzyme
704 combinations to break down glycans, Nat. Commun. 10 (2019) 2043. [https://doi.org/10.1038/s41467-](https://doi.org/10.1038/s41467-019-10068-5)
705 [019-10068-5](https://doi.org/10.1038/s41467-019-10068-5)
- 706 [55] R. Jumpertz, D. Le, P. Turnbaugh, C. Trinidad, C. Bogardus, J. Gordon, J. Krakoff, Energy-balance
707 studies reveal associations between gut microbes, caloric load, and nutrient absorption in humans, Am.
708 J. Clin. Nutr. 94 (2011) 58–65. <https://doi.org/10.3945/ajcn.110.010132>
- 709 [56] R. Szava-Kovats, M. Pärtel, Biodiversity Patterns along ecological gradients: Unifying β -diversity
710 indices, PLoS One 9 (2014) e110485. <https://doi.org/10.1371/journal.pone.0110485>
- 711 [57] Y. Chung, Y. Ryu, B. An, Y. Yoon, O. Choi, T. Kim, J. Yoon, J. Ahn, H. Park, S. Kwon, J. Kim, M.
712 Chung, A synthetic probiotic engineered for colorectal cancer therapy modulates gut microbiota,
713 Microbiome 9 (2021) 122. <https://doi.org/10.1186/s40168-021-01071-4>
- 714 [58] A. Koh, F. De Vadder, P. Kovatcheva-Datchary, F. Bäckhed, From dietary fiber to host physiology:
715 short-chain fatty acids as key bacterial metabolites, Cell 165 (2016) 1332–1345.
716 <https://doi.org/10.1016/j.cell.2016.05.041>
- 717 [59] T. Aziz, A. Sarwar, Z. Daudzai, J. Naseeb, J.U. Din, U. Aftab, A. Saidal, M. Ghani, A.A. Khan, S. Naz,
718 M. Shahzad, H. Cui, L. Lin, Conjugated fatty acids (CFAs) production via various bacterial strains and
719 their applications. A review, J. Chil. Chem. Soc. 67 (2022) 5445–5452. [https://doi.org/10.4067/S0717-](https://doi.org/10.4067/S0717-97072022000105445)
720 [97072022000105445](https://doi.org/10.4067/S0717-97072022000105445)
- 721 [60] X. Xiang, R. Wang, L. Chen, Y. Chen, B. Zheng, S. Deng, S. Liu, P. Sun, G. Shen, Immunomodulatory
722 activity of a water-soluble polysaccharide extracted from mussel on cyclophosphamide-induced

723 immunosuppressive mice models, *Npj Sci. Food* 6 (2022) 26. <https://doi.org/10.1038/s41538-022->
724 00140-8
725

726 **Tables**

727 **Table 1.** Effects of EPS on DTH and phagocytic index in CTX-induced immunosuppressive
728 mice.

Group	Toe thickness (mm)	Phagocytic index
NC	0.588±0.095 ^a	5.33±0.14 ^a
MC	0.708±0.115 ^e	4.32±0.16 ^c
LD	0.674±0.078 ^d	4.56±0.18 ^c
MD	0.636±0.121 ^{cd}	4.92±0.11 ^b
HD	0.581±0.100 ^{ab}	5.21±0.09 ^a
PC	0.615±0.070 ^{bc}	5.29±0.20 ^a

729 Note: The different lowercase letters mean the significant difference between the groups
730 ($P<0.05$).

731 **Table 2.** Effects of EPS on spleen index, thymus index and proliferation rate of
 732 splenic lymphocytes in CTX-induced immunosuppressive mice

Group	Spleen index	Thymus index	Proliferation rate of splenic lymphocytes (%)
NC	0.410±0.030 ^a	0.283±0.042 ^a	100±4.68 ^a
MC	0.307±0.050 ^c	0.187±0.056 ^c	49.04±4.78 ^c
LD	0.331±0.053 ^{bc}	0.211±0.043 ^{bc}	50.66±7.08 ^c
MD	0.356±0.044 ^{abc}	0.245±0.059 ^{abc}	64.68±6.30 ^b
HD	0.397±0.07 ^{ab}	0.287±0.030 ^a	76.97±3.33 ^a
PC	0.390±0.07 ^{ab}	0.267±0.065 ^{ab}	75.21±4.22 ^a

733 Note: The different lowercase letters mean the significant difference between the groups
 734 ($P < 0.05$).

735 **Table 3.** Effects of EPS on the HC₅₀ value and content of cytokines in serum of CTX-induced
 736 immunosuppressive mice

Group	HC ₅₀ (pg mL ⁻¹)	IFN-γ (pg mL ⁻¹)	TNF-α (pg mL ⁻¹)	IL-10 (pg mL ⁻¹)
NC	246.39±28.65 ^a	32.16±1.87 ^a	28.32±2.05 ^a	47.08±1.28 ^a
MC	125.61±15.47 ^c	20.18±2.09 ^d	15.68±1.32 ^d	34.17±1.14 ^e
LD	137.45±21.25 ^c	23.79±1.23 ^d	17.89±1.29 ^{cd}	36.18±2.07 ^{de}
MD	187.25±17.65 ^b	26.08±1.57 ^c	20.18±2.08 ^{bc}	39.96±1.78 ^{cd}
HD	231.75±26.95 ^a	30.34±1.47 ^{ab}	24.99±1.61 ^a	45.69±1.82 ^b
PC	214.75±22.65 ^{ab}	28.43±1.66 ^b	22.32±2.18 ^{ab}	43.12±1.69 ^{bc}

737 Note: The different lowercase letters mean the significant difference between the groups
 738 ($P < 0.05$).

739

740 **Figure Captions**

741 **Fig. 1.** Animal experimental protocol and design of this study.

742 **Fig. 2.** Effects of EPS on body weight. The different lowercase letters indicate the significant
743 difference between the groups ($P<0.05$).

744 **Fig. 3.** Morphological images of mouse organs and tissues. (A) Spleens; (B) Colon; (C) Section
745 of thymus; (D) Sections of duodenum, jejunum, ileum, and colon. The different lowercase
746 letters labeled on the numerical value of image A and B indicate the significant difference
747 between the groups ($P<0.05$). The lowercase letters a-f in each image represent NC, MC, LD,
748 MD, HD, and PC groups, respectively.

749 **Fig. 4.** Effect of TLR4 inhibitor TAK-242 (A) and MAPKs inhibitors CI-1040, SP600125, and
750 SB239063 (B) on NO, TNF- α , IL-1 β , and IL-6 secretion of RAW 264.7 cells induced by LPS
751 or EPS.

752 **Fig. 5.** (A) Shannon Wiener rarefaction curve (a) and Rank-Abundance curve (b) of mice
753 intestinal flora; (B) Venn diagram of mouse intestinal flora on OTU level; (C) Alpha diversity
754 indices, (a) Chao index, (b) Ace index, (c) Shannon Wiener index, (d) Simpson index. The
755 capital letters A-D in each figure represent the MC, HD, PC, and NC groups, respectively.

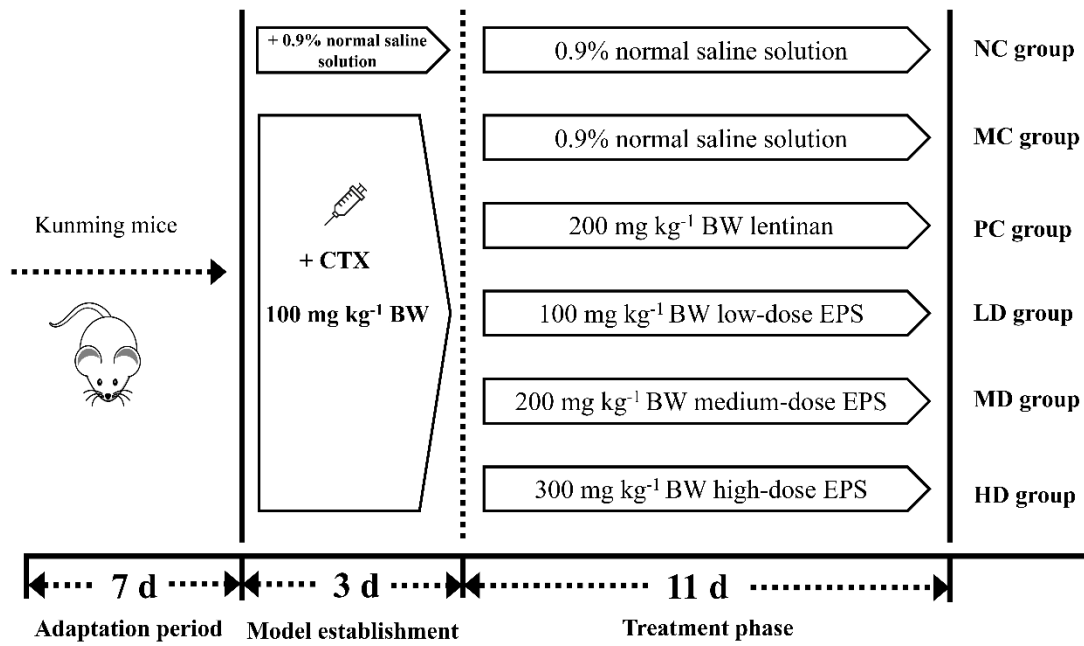
756 **Fig. 6.** Composition of intestinal flora in mice at phylum (A) and family (B) levels. The capital
757 letters A-D in each figure represent the MC, HD, PC, and NC groups, respectively.

758 **Fig. 7.** (A) Sample distances heatmap on OTU level; (B) PCoA analysis of intestinal flora of
759 mice; (C) LEfSe analysis of intestinal flora in different treatment groups, (a) MC vs NC, (b)
760 MC vs HD, (c) HD vs NC, (d) HD vs PC. The capital letters A-D in each figure represent MC,
761 HD, PC, and NC groups, respectively.

762 **Fig. 8.** The contents of SCFAs in mouse feces; (B) RDA analysis of environmental factors at
763 OTU level; (C) Classification of COG prediction function of mouse intestinal flora. The capital
764 letters A-D in each figure represent MC, HD, PC, and NC groups, respectively.
765

766 **Fig. 1**

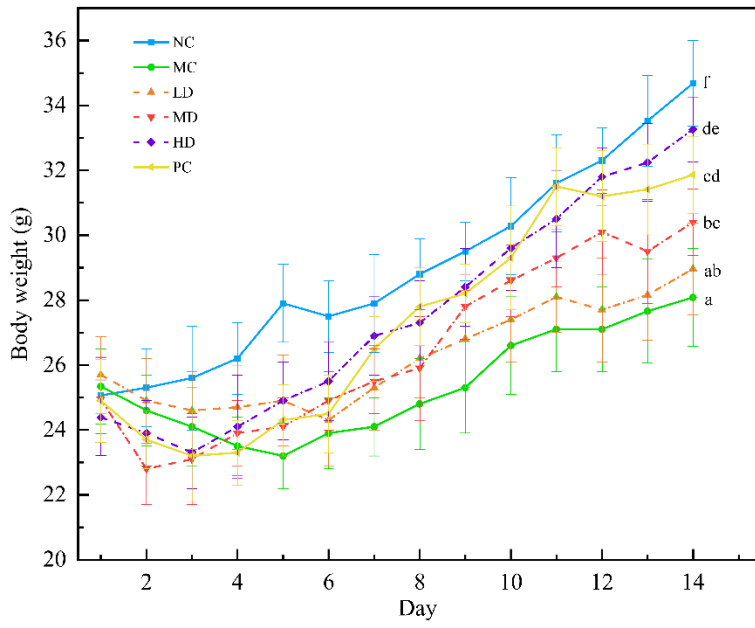
767



768

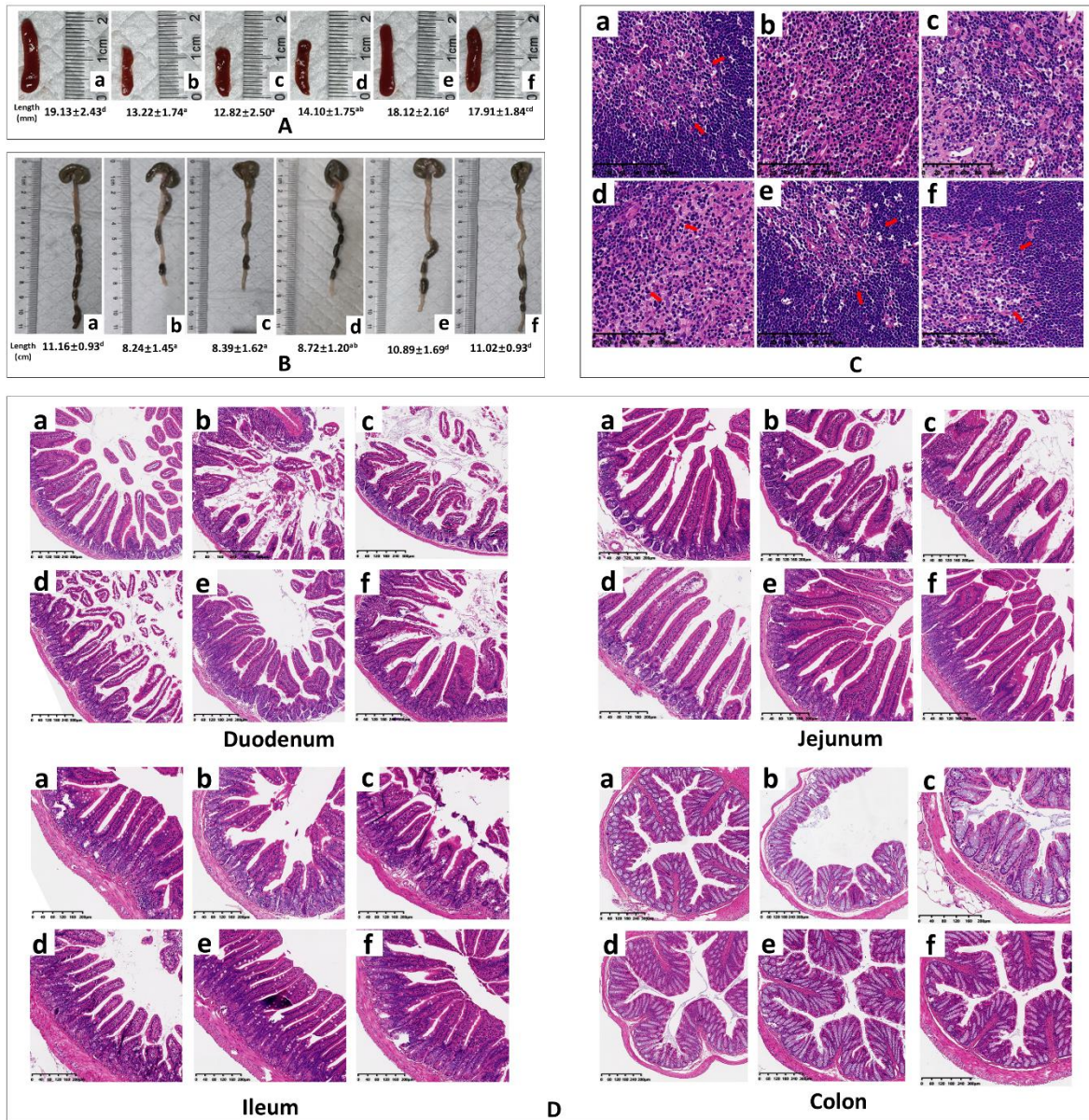
769

770 **Fig. 2**



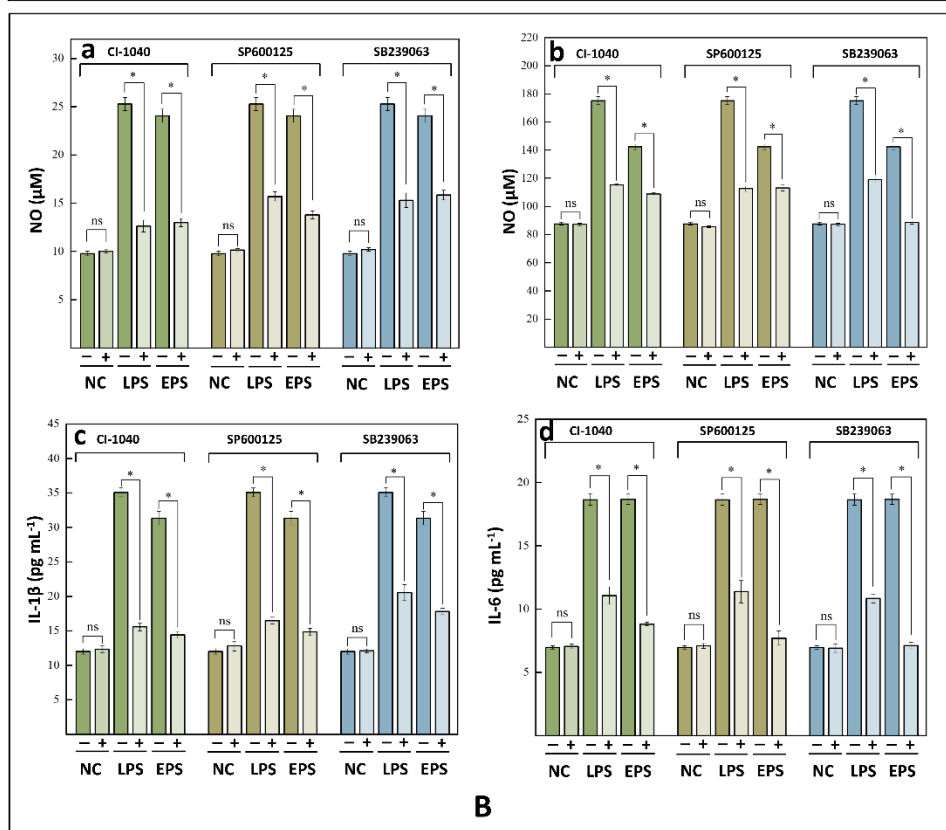
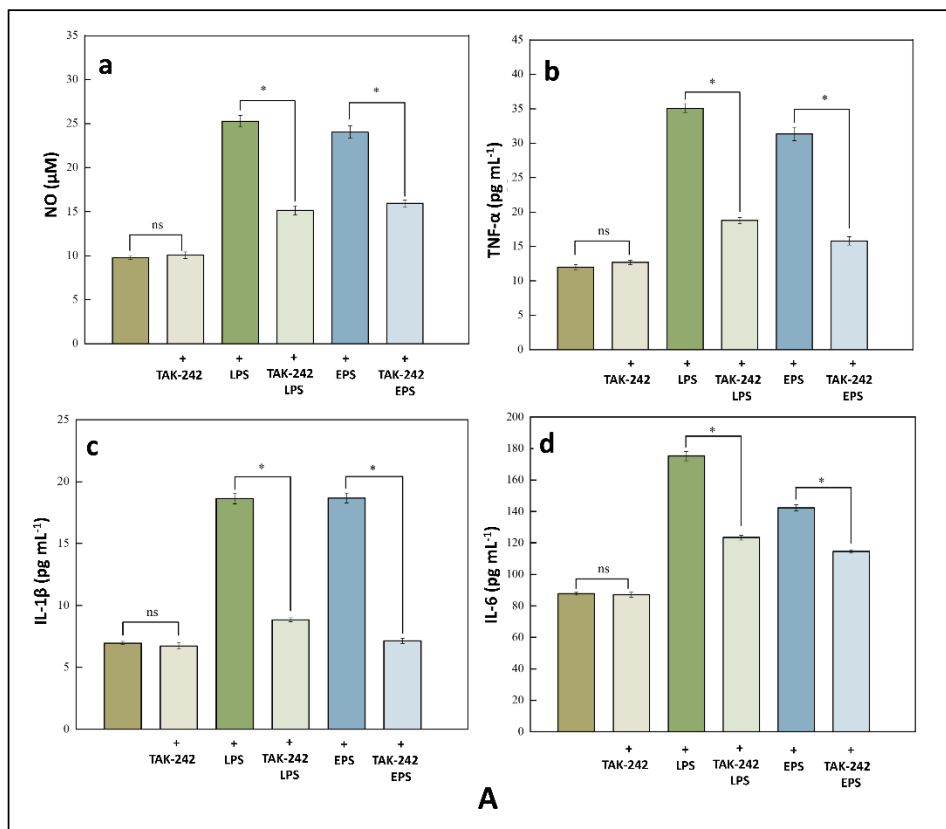
771

772

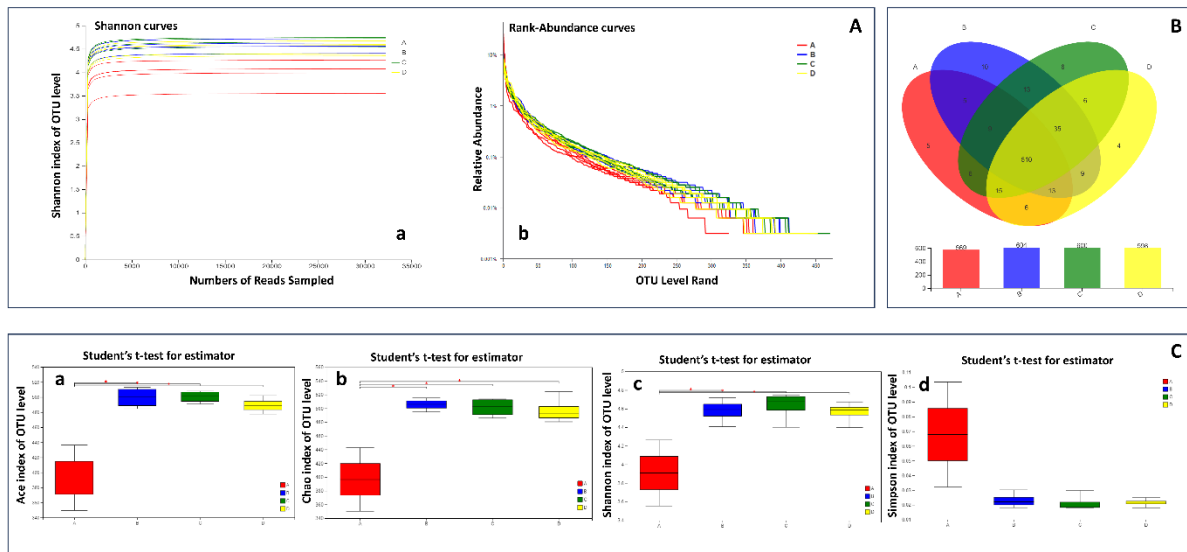


774

775



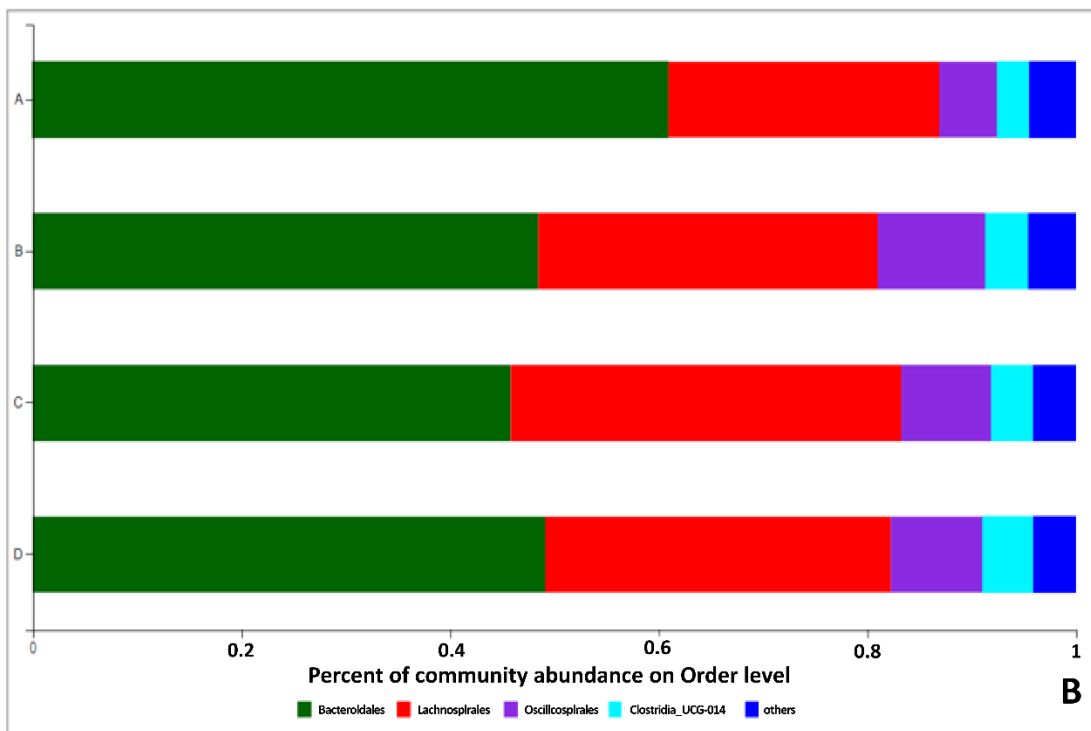
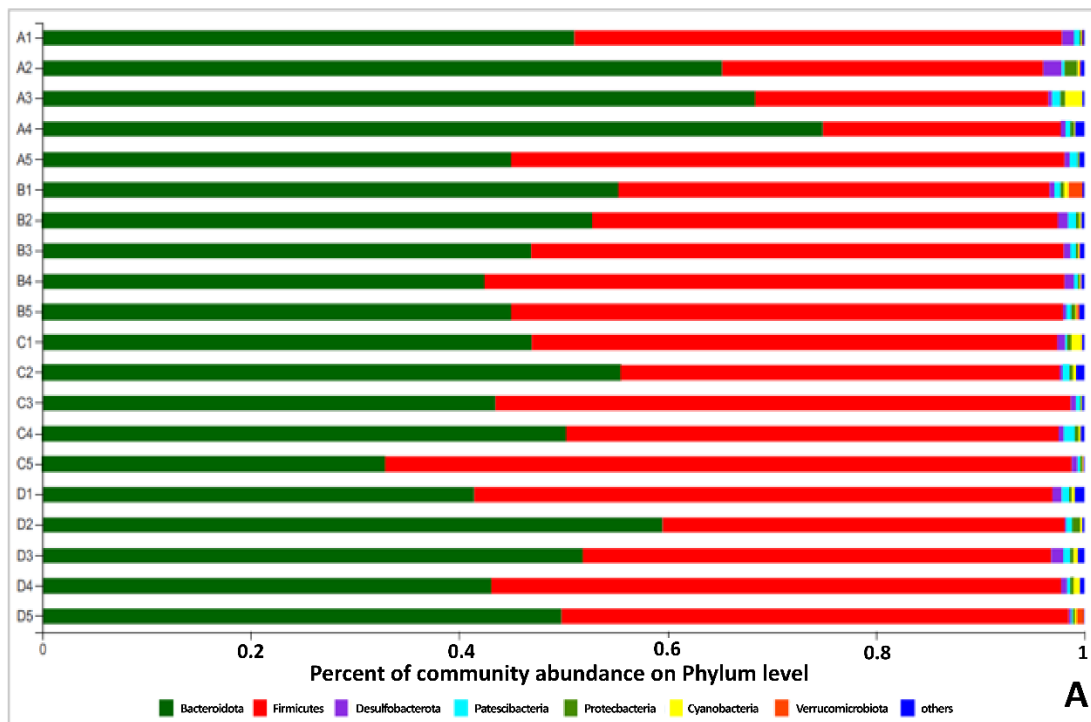
779 **Fig. 5**



780

781

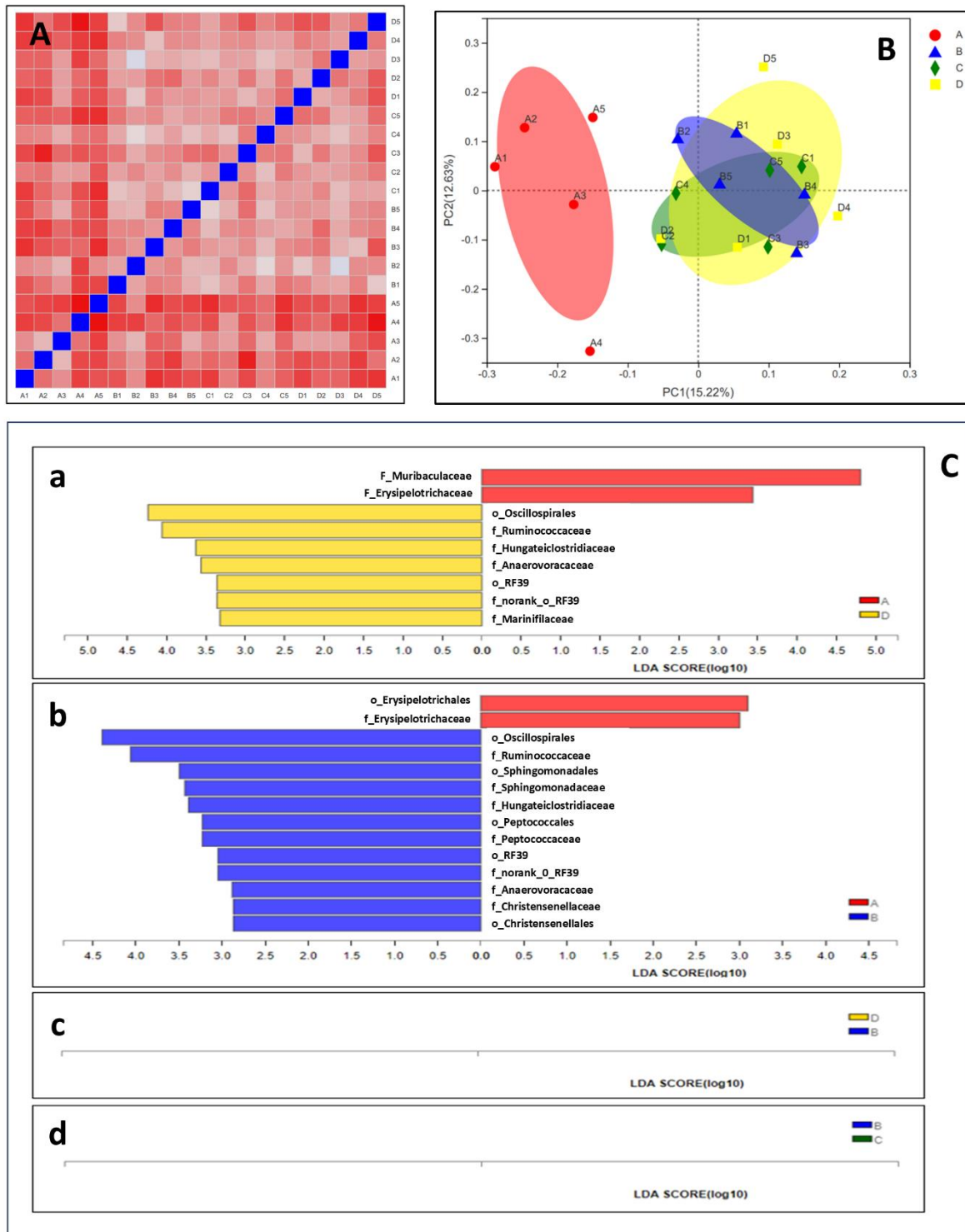
782 **Fig. 6**



783

784

785 Fig. 7



786

787

